Hindawi Publishing Corporation
International Journal of Photoenergy
Volume 2013, Article ID 276504, 8 pages
http://dx.doi.org/10.1155/2013/276504

Research Article

Single Step Formation of C-TiO_2 Nanotubes: Influence of Applied Voltage and Their Photocatalytic Activity under Solar Illumination

Chin Wei Lai[1] and Srimala Sreekantan[2]

[1] *Nanotechnology & Catalysis Research Centre (NANOCAT), Institute of Postgraduate Studies (IPS), Universiti Malaya, 3rd Floor, Block A, 50603 Kuala Lumpur, Malaysia*
[2] *School of Materials and Mineral Resources Engineering, Universiti Sains Malaysia Engineering Campus, Seberang Perai Selatan, Pulau Pinang, 14300 Nibong Tebal, Malaysia*

Correspondence should be addressed to Chin Wei Lai; cwlai@um.edu.my

Received 25 June 2013; Revised 29 September 2013; Accepted 7 October 2013

Academic Editor: Huogen Yu

Self-aligned and high-uniformity carbon (C)- titania (TiO_2) nanotube arrays were successfully formed via single step anodization of titanium (Ti) foil at 30 V for 1 h in a bath composed of ethylene glycol (EG), ammonium fluoride (NH_4F), and hydrogen peroxide (H_2O_2). It was well established that applied voltage played an important role in controlling field-assisted oxidation and field-assisted dissolution during electrochemical anodization process. Therefore, the influences of applied voltage on the formation of C-TiO_2 nanotube arrays were discussed. It was found that a minimal applied voltage of 30 V was required to form the self-aligned and high-uniformity C-TiO_2 nanotube arrays with diameter of ~75 nm and length of ~2 μm. The samples synthesized using different applied voltages were then subjected to heat treatment for the conversion of amorphous phase to crystalline phase. The photocatalytic activity evaluation of C-TiO_2 samples was made under degradation of organic dye (methyl orange (MO) solution). The results revealed that controlled nanoarchitecture C-TiO_2 photocatalyst led to a significant enhancement in photocatalytic activity due to the creation of more specific active surface areas for incident photons absorption from the solar illumination.

1. Introduction

Nowadays, various kinds of environmental contaminants are around all of us, especially organic and inorganic pollutants from industrial wastewaters [1–3]. Thus, the treatments of such wastewater have become a major concern and it is urgent to develop a sustainable and cost-effective treatment technology to solve global environmental problems [3, 4]. In recent years, the photocatalyst system has attracted much attention from science community as one of the most promising ways to solve the environmental problems [4–6]. This system is considered to be an ideal and green environmental solution for our green economy future.

In this case, TiO_2 based nanomaterials have been broadly studied as the most promising photocatalyst for environmental remediation such as air purification, water purification, heavy metals degradation, and hazardous waste remediation [6–10]. The reasons are mainly attributed to the non-toxicity, cost-effectiveness, long-term stability, widespread availability, and high stability against photocorrosion with great capacity for oxidation and high photocatalytic property. To date, development of nanoarchitecture of TiO_2 assemblies with precisely controllable nanoscale features has gained significant scientific interest [11, 12]. Among different nanoarchitectures of TiO_2, one-dimensional (1D) TiO_2 is considered as a promising candidate in environmental and industrial pollutants degradation due to the well controllable dimensional features such as pore diameter, length, and wall thickness [6–9, 11–15]. However, its practical application was limited by poor absorption of photons from the solar illumination and high recombination losses of photoinduced electron-hole pairs [1, 4, 10, 16–18].

Recently, numerous research studies have been paid for the rational design of high efficiency heterostructure C-TiO_2 based nanomaterial for remarkable solar absorption and higher separation efficiency of photo-induced charge carriers [4, 19–22]. In particular, C-TiO_2 based nanomaterials can exert a substantial influence on modifying electronic structure and the construction of heterotomic surface structure that allow higher efficiency photocatalysis reaction under solar irradiation [19, 21, 23]. Several literatures have reported that incorporation of anion C-dopants into TiO_2 crystalline could shift its photoresponse into visible region, which accounts for 40–45% irradiation from the solar light. The main reason was attributed to the narrowing of the band gap energy, which resulted from an increase in the width of the valence band. The reduction of band gap energy was believed to be from the mixing of the p-state of C dopants with O $2p$ and Ti $3d$ orbital constituting valence band [21, 23, 24].

In the present study, a detailed study on the C-doped TiO_2 nanotubes via single step of electrochemical anodization technique was performed. An organic electrolyte of ethylene glycol was selected as C source to dope into TiO_2 nanotubes during electrochemical anodization. This study aims to determine the minimal applied voltage to grow the self-aligned and high-uniformity C-TiO_2 nanotubes for better photocatalytic performance. The novelty of this work is to synthesize a potential photocatalyzer, which shows strong absorption range in UV-visible region, strong oxidation ability, cost-effective and time saving process.

2. Experimental Procedure

2.1. Preparation of Anodic C-TiO_2 Nanotubes. 99.6% purity of Ti foils (Strem Chemical, USA) with dimension of 50 mm × 10 mm × 0.127 mm was used in this experimental study. The electrochemical anodization process was performed in an organic electrolyte of EG ($C_2H_6O_2$, >99.5%, Merck, USA), 5 wt% of NH_4F (98%, Merck, USA), and 5 wt% of H_2O_2 (30% H_2O_2 : 70% H_2O, J.T. Baker, USA). This composition was selected because it favors the formation of well-aligned and highly ordered nanotubular structure based on our previous studies [25]. Electrochemical anodization process was conducted for 1 h with three different applied voltages (e.g., 10 V, 20 V, and 30 V). Anodization was performed in a two-electrode configuration bath with Ti foil as the anode and a platinum rod as the cathode. Subsequently, these samples were annealed at 400°C for 4 h in an argon atmosphere.

2.2. Characterization of Anodic C-TiO_2 Nanotubes. The Field Emission Scanning Electron Microscopy (FESEM) and Energy Dispersive X-Ray (EDX) were conducted (FEI Quanta 200 FESEM model, USA). The cross-sectional measurements were carried out on mechanically bent samples, where a partial lift-off of the anodic layer occurred to obtain the thickness of the anodic oxide formed on Ti foil. The crystalline phase of the synthesized samples was identified by power X-ray Diffraction (XRD), using a Bruker X-ray Diffraction Model D-8, USA, equipped with a Cu Kα monochromatized radiation source (λ = 1.5406 Å). The sample with dimension (10 mm × 10 mm) was placed onto a specimen holder and then placed in the rotating unit stage of diffractometer system. The data was collected within 2θ of 10° to 70° with a step size of 0.034° at scan time 71.6 sec. Photoluminescence (PL) spectra were obtained at room temperature using an LS 55 luminescence spectrometer (Jobin-Yvon HR 800UV). The photoelectron spectra were obtained through X-ray photoelectron spectroscopy (XPS; JEOL JPS-1000SX) with a dual X-ray source, in which an Al-Kα (30 kV) anode and a hemispherical energy analyzer were used. The background pressure during data acquisition was maintained at 7.0×10^{-9} Torr. All binding energies were calibrated using contaminant carbon (C1s = 284.8 eV) as a charge reference.

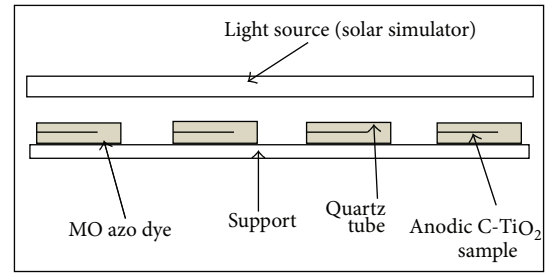

Figure 1: Schematic diagram of the experimental setup for quartz glass tube custom-made photoreactor used in photocatalytic degradation MO dye studies.

2.3. Photocatalytic Degradation of MO Dye Study. Photocatalytic degradation MO dye was conducted by dipping 4 cm^2 of anodic C-TiO_2 nanotubes samples into a 100 mL of quartz glass tube containing 30 ppm of MO dye. The quartz glass tube was then placed in a custom-made photo-recator for photocatalytic degradation studies. A schematic diagram of quartz glass tube custom-made photo-reactor used in photocatalytic degradation MO dye is exhibited in Figure 1. In this study, a blank sample (without anodic sample) was prepared in order to eliminate the effect of light towards the degradation of MO dye solution. All anodic samples were left in a custom-made photo-reactor for 30 min in dark environment to achieve adsorption and desorption equilibrium. Then, samples were photoirradiated using a 150 W Xenon solar simulator (Zolix LSP-X150, China) with intensity of 800 W/m^2. Three mL of MO dye solution was withdrawn from the quartz glass tube every 1 h to investigate the degradation of MO dye solution under solar irradiation. The concentration of the degraded MO dye solution assisted by the anodic sample was determined using UV-Vis spectrometer (PerkinElmer Lambda 35, USA).

3. Results and Discussion

3.1. Surface Morphology of Anodic C-TiO_2 Nanotubes. The effect of applied voltage in an organic electrolyte of EG solution containing 5 wt% of NH_4F and 5 wt% of H_2O_2 on the morphology of the self-organized TiO_2 nanotubes

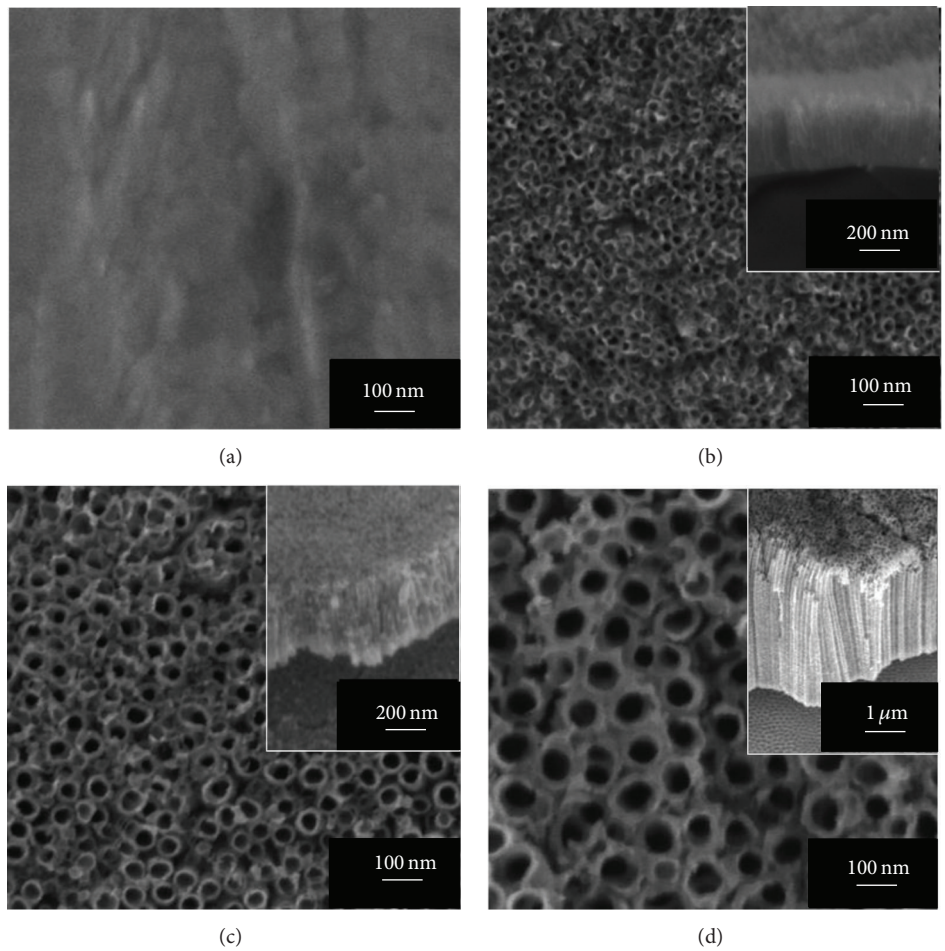

FIGURE 2: FEESEM images of (a) pure Ti foil and C-TiO_2 nanotube arrays fabricated at different applied voltage in an EG electrolyte containing 5 wt% of NH_4F and 5 wt% of H_2O_2 for 1 h at (b) 10 V, (c) 20 V, and (d) 30 V (inset: cross-sectional view).

is discussed. Based on our preliminary study, an optimum content of 5 wt% H_2O_2 played an important role in increasing the oxidation rate of Ti to form TiO_2, while 5 wt% of NH_4F was sufficient to trigger the chemical dissolution reaction to form nanotubular structure during electrochemical anodization [25–27]. The morphology of the Ti foil before conducting electrochemical anodization was characterized by FESEM (Figure 2(a)). It is clearly shown that Ti foil was flat without any pits or pores on its surface. The oxide layer has not yet been formed. The FESEM micrographs of the synthesized nanostructures of anodic C-TiO_2 samples after electrochemical anodization varied from 10 V to 30 V are shown in Figure 2(b) to Figure 2(d). The inset micrographs show the cross-sectional morphology of oxide layer on the anodized Ti foil. These FESEM micrographs clearly show that the applied voltage affects the geometric features are the appearance of the nanotubular structure on the Ti foils. It could be observed that anodized samples exhibited uniform growth of nanotube arrays throughout the surface of Ti foil. The surface and inset of cross-sectional morphology of the Ti foil anodized at a lower applied voltage of 10 V are shown in Figure 2(b). It was found that an average of 25 nm diameters and an average thickness of 550 nm of nanotube arrays were produced. Upon increasing the applied voltage to 20 V, the average diameter for the nanotubular structure was increased to 45 nm with thickness of 750 nm (Figure 2(c)). It is noteworthy to mention that uniform circular nanotube arrays were successfully formed when minimum voltage of 30 V was applied during electrochemical anodization. The average diameter of 80 nm and thickness of 2 μm nanotubes were produced (Figure 2(d)). Therefore, uniform growth of anodic nanotube arrays at lower 30 V of applied voltage was selected and duplicated for the investigation studies.

3.2. Chemical Compositions of Anodic C-TiO_2 Nanotubes. EDX analysis was employed to investigate the chemical stoichiometry of the anodic C-TiO_2 nanotubes after heating treatment at 400°C in argon atmosphere. As determined through EDX analysis, the anodic C-TiO_2 nanotubes synthesized at 30 V consisted of 60.14 at% of Ti element, 33.68 at% of O element and 6.18 at% of C element (Figure 3). An additional spectrum of C was observed at about 0.2 keV from the EDX spectra. This result showed the presence of C species in anodic TiO_2 nanotubes. The main reason is favorable to the oxidation of organic EG electrolyte to carbonate type

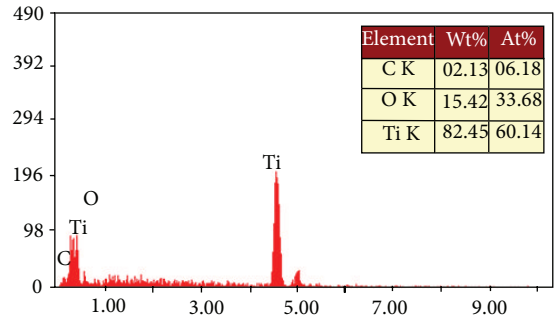

Figure 3: EDX spectra of self-aligned and high-uniformity C-TiO_2 nanotube arrays formed in an EG electrolyte containing 5 wt% of NH_4F and 5 wt% of H_2O_2 for 1 h at 30 V.

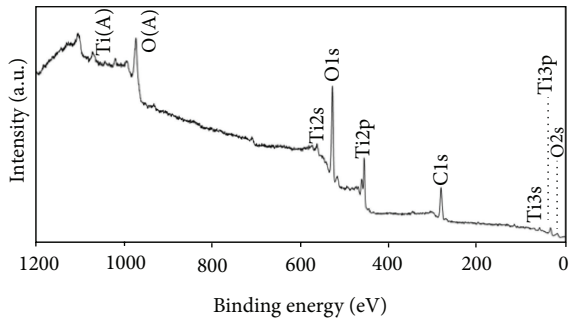

Figure 4: XPS survey spectra of self-aligned and high-uniformity C-TiO_2 nanotube arrays formed in an EG electrolyte containing 5 wt% of NH_4F and 5 wt% of H_2O_2 for 1 h at 30 V.

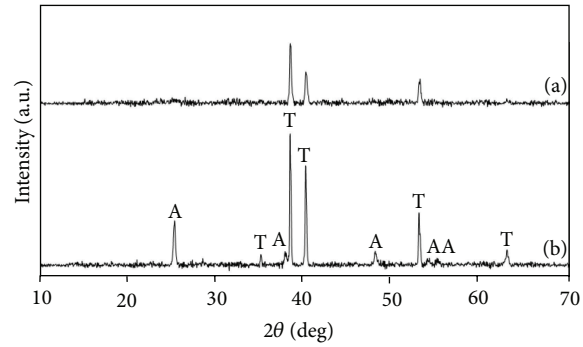

Figure 5: XRD pattern of self-aligned and high-uniformity C-TiO_2 nanotube arrays formed in an EG electrolyte containing 5 wt% of NH_4F and 5 wt% of H_2O_2 for 1 h at 30 V, (a) as-anodized and (b) annealed at 400°C under argon atmosphere for 4 h (Ti: titanium; A: anatase).

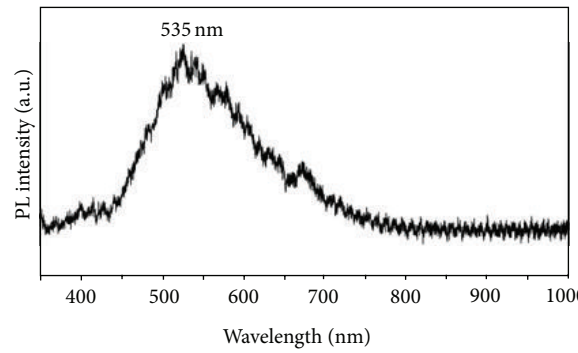

Figure 6: The PL emission spectra of self-aligned and high-uniformity C-TiO_2 nanotube arrays formed in an EG electrolyte containing 5 wt% of NH_4F and 5 wt% of H_2O_2 for 1 h at 30 V.

species which gets absorbed on the wall of nanotubes during the electrochemical anodization [19, 24, 28]. These resultant carbonate type species were reduced to C species during heat treatment process and diffused into the TiO_2 lattice [29]. In this manner, the single step incorporation of C species to TiO_2 nanotubes could be achieved.

Next, XPS measurements were carried out to further investigate the chemical composition and oxidation state of C-TiO_2 nanotubes. XPS survey spectra for the sample synthesized at 30 V are presented in Figure 4. The elements of Ti, O, and C were detected from the XPS survey spectra, which indicated that the carbon species were successfully loaded into the lattice of TiO_2. It was found that the peak of Ti2p (binding energy of about 460 eV) is attributed to Ti^{4+}. Besides, it could be observed that the peak of O1s (binding energy of about 530 eV) showed the presence of oxygen atoms in the TiO_2 structure. Meanwhile, the detection of the peak C1s at about 285 eV can be ascribed to the Ti–C–O bonds of the carbonate species originating from the residual carbon of the organic ethylene glycol electrolyte.

3.3. Crystalline Structure of Anodic C-TiO_2 Nanotubes. In the present study, XRD measurements were conducted to reveal the crystal phase transition of the as-anodized and annealed samples. The results are presented in Figure 5. Based on preliminary study, 400°C was sufficient to convert TiO_2 amorphous structure to high crystallinity of anatase phase, which exhibited thermodynamically stable and higher surface stability [30–33]. It was found that the presence of Ti phase only was detected from the XRD pattern for the as-anodized sample, which represents the amorphous phase of TiO_2 (Figure 5(a)). However, high crystallinity of anatase phase was detected for the sample subjected to annealing at 400°C in argon atmosphere (Figure 5(b)). It can be seen that the diffraction peaks of the entire samples are ascribed to the TiO_2 with anatase phase (JCPDS no. 21–1272). The diffraction peaks allocated at 25.37°, 38.67°, 48.21°, 54.10°, and 55.26° are corresponding to (101), (112), (200), (105), and (211) crystal planes for the anatase phase, respectively.

3.4. Optical Property of Anodic C-TiO_2 Nanotubes. PL emission spectra were broadly used to investigate the competency of charge carrier trapping, migration, and transfer behaviors of anodic C-TiO_2 nanotubes. The information from PL emission spectra is important to understand the state of electron-hole pairs in C-TiO_2 nanotubes photocatalyst since the emission mainly resulted from recombination dynamics of these free carriers. The PL measurement was conducted at room temperatures in the wavelength range of 350 nm to 1000 nm as presented in Figure 6. The dominant PL emission

spectrum of the samples prepared at 30 V is clearly observed at 535 nm, implying the visible-light characteristics of the sample. The dominant PL spectrum of anatase phase TiO_2 was closely related to the recombination of self-trapped excitons localized on the TiO_6 octahedral, which results from the interaction of the negative electrons located in the Ti $3d$ states with the positive holes in the O $2p$ state [7, 16, 19]. In this case, the peak position at 535 nm might be attributed to the radioactive recombination of self-trapped excitons localized on TiO_6 octahedron. On the other hand, the PL emissions above 535 nm might be attributed to the presence of surface state and intrinsic defects such as oxygen vacancies, which give rise to donor states located below conduction band. Several literatures have reported that the resultant PL emission spectra were attributed to the oxygen-related defects within the sample lattice [34, 35]. Zhao and co-workers have been reported that the carbon species doping into the lattice of TiO_2 nanotubes favored the formation of oxygen vacancies [36]. They proposed that the electrons were easily trapped by those oxygen vacancies, while the holes were trapped by carbon species. This condition could decrease the PL intensity significantly. Hence, the presence of carbon species could improve the separation extent and restrain the recombination losses of the photo-induced charge carriers. Besides, PL technique has been widely used to investigate the energy levels of samples [23, 37]. The energy level (E_b) of the samples was calculated using the equation $E_b = hc/\lambda$, where E_b is the band gap energy, h is Planck's constant (4.135667×10^{-15} eV s), c is the velocity of light (2.997924×108 m/s), and λ is the wavelength (nm) of PL emission. The E_b was found at around 2.3 eV, which is relatively low as compared to the E_b of pure TiO_2 (3.2 eV for anatase phase) [7, 10]. The result clearly demonstrates that visible emission is likely facilitated by the interstitial C species within the lattice of TiO_2.

3.5. Formation Mechanism of Anodic C-TiO_2 Nanotubes. In the present study, applied voltage played an important role in controlling the field-assisted oxidation of Ti metal to form TiO_2 and field-assisted dissolution of Ti metal ions into electrolyte [38, 39]. A simple schematic illustration about the formation mechanism of anodic C-TiO_2 nanotube arrays was presented in Figure 7. The compact oxide layer was formed through the hydrolysis of Ti foil (stage A) which was oxidized to TiO_2 forming a barrier type layer under applied voltage. This layer grew predominantly by the inward migration of oxygen ions (O^{2-}) through this layer toward Ti/TiO_2 interface with further growth of barrier layer (stage B). The high electric field across the oxide layer subsequently induced the polarization of Ti–O bonding. In this manner, Ti^{4+} ions from the barrier layer of TiO_2 will dissolve into the electrolyte and form pits randomly on the surface of oxide layer. The pits will act as nucleation sites for the porosification (stage C). The titanium-fluoro complexes $(TiF_6)^{2-}$ will induce the chemical dissolution and continuous dissolve the pits, which will further enlarge and deepenly the pits into nanotubular structure. The rate of migration of the Ti^{4+}, O_{2-}, and F^- ions was higher during the higher voltage electrochemical anodization. The higher electron flow promoted increased

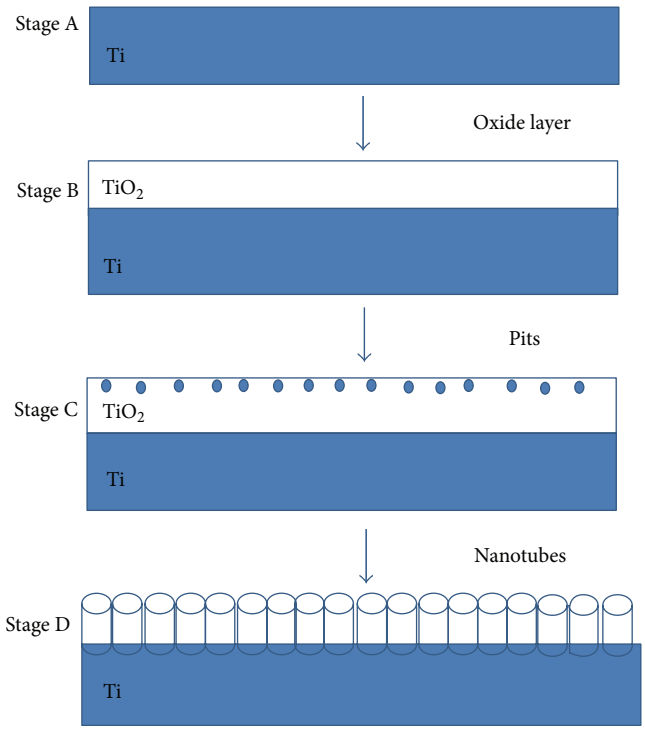

Figure 7: Schematic illustration for the formation mechanism of anodic C-TiO_2 nanotube arrays via electrochemical anodization technique.

field-assisted oxidation and field-assisted dissolution, which leads to an increase in nanotube length and pore size (stage D). The porosity will reach a steady-state, resulting in the formation of uniform of TiO_2 nanotubes [9, 11, 26].

In this manner, organic EG electrolyte was oxidized to carbonate-species under applied voltage, which get absorbed on the wall of nanotubes. Then, these carbonate-species were reduced to C species during annealing treatment process, which might diffuse into the lattice of TiO_2 [29]. Thus, the presence of the C species was found within TiO_2 nanotubes. Valentin and coworkers have proposed that the possible causes for the presence of C atoms in the anatase TiO_2 are due to the substitution of the oxygen lattice with a C atom, the replacement of Ti atoms with a C atom; and stabilization of a C atom at interstitial position of TiO_2 lattice [21]. As a matter of fact, the interstitial C atom arises from the pyrogeneration of EG electrolyte, which reduces the band gap marginally or to introduce mid-gap level to increase the light absorption into visible region. In this case, the band gap level reduction was believed to result from an increase in the width of the valence band due to the mixing of the delocalized p-state of carbon dopants with O $2p$. The mixing p-state of the C dopants with $2p$ of O will shift the valence band edge upwards (~0.8 eV above the valence band) to narrow down the band gap of TiO_2 to ~2.3 eV [11, 19]. A comparison between the pure TiO_2 and C-TiO_2 under solar irradiation for the photo-induced electrons transfer pathways was exhibited in Figure 8. Thus, electronic coupling of these states with electronic

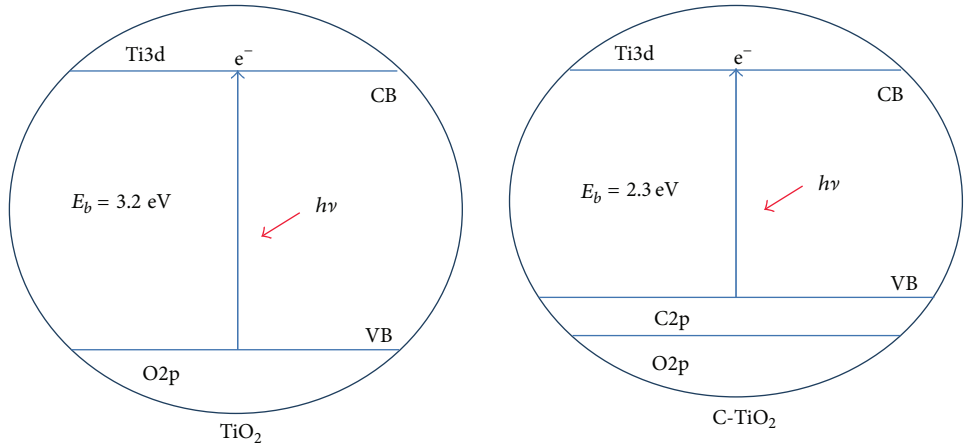

FIGURE 8: The comparison of the photo-induced electrons transfers pathways for pure TiO_2 and C-TiO_2 under solar irradiation.

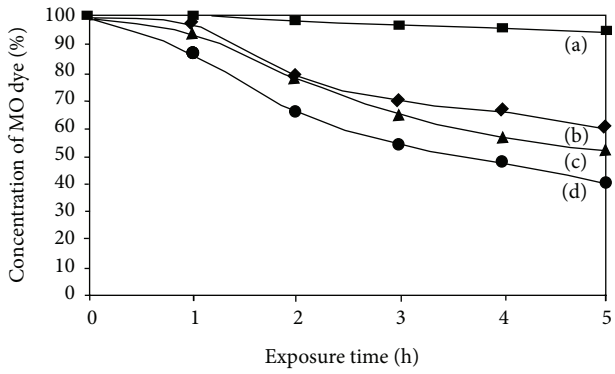

FIGURE 9: Photodegradation of MO dye solution under solar illumination. (a) Blank sample (without anodic sample); samples of C-TiO_2 nanotube arrays produced at (b) 10 V, (c) 20 V, and (d) 30 V.

continuum of TiO_2 valence band state yields a band of surface state at where the electrons could be generated in conduction band by low energy of visible light irradiation [23].

3.6. Photocatalytic Decolorization of MO Dye Evaluation. The significance of C-TiO_2 nanotubes from different applied voltages (10 V–30 V) was applied as the photocatalytic performance evaluation by decolorization of MO dye under visible light irradiation. Figure 9 clearly shows the continuous decrease in the concentration of MO dyes with increasing exposure time. It was found that the decolorization of MO dye follows an apparent first-order kinetic reaction. The decolorization rate order was C-TiO_2-30 V > C-TiO_2-20 V > C-TiO_2-10 V. It could be observed that the C-TiO_2-30 V exhibited the highest photocatalytic performance of ~60% after exposure to solar irradiation for 5 h. The dominating factor in decolorization of MO dye is attributed to the active surface area of the catalyst to absorb more photons from the solar irradiation [40, 41]. In addition, higher active surface area will allow more organic MO molecules to absorb onto the C-TiO_2 surface. Furthermore, higher uniformity of nanotube arrays will result in more rapid diffusion of the organic MO molecules into the inner of nanotubes for photocatalytic reaction [41, 42]. In this case, C content within the nanotubes could play an important role in reducing the band gap energy of TiO_2 nanotubes (from 3.2 eV to 2.3 eV based on the anatase phase). The visible emission is likely facilitated by the interstitial C species within the lattice of TiO_2. Thus, the photo-induced charge carriers could be generated effectively under solar illumination. Besides, the photo-induced electrons were easily trapped by this C content and led to higher transportation of charge carriers from bulk to surface of TiO_2, which retards the recombination losses. It is a well-known fact that MO molecule has one $-SO_3^-$ group and two alkyl groups ($-CH_3$), which can improve the adsorption of the H_2O or OH^- ions on C-TiO_2 surface [43]. In this manner, C-TiO_2 nanotubes play an essential role in promoting the adsorption of OH species on the inner and outer wall surface of nanotubes and consequently promoting the photocatalytic reaction.

In the present study, photocatalytic reaction in decolorization of MO dye strongly depends on the ability of catalyst to create photo-induced charge carriers, which generate free radicals (hydroxyl radicals of $^{\bullet}OH$) able to undergo secondary reactions [6, 8, 9]. Theoretically, the exposure of a photocatalyst to irradiation ($h\nu$) higher than its E_b will result in the transition of photo-induced electrons (e^-) from the O $2p$ state to the Ti $3d$ state and leave behind photo-induced holes (h^+). Nevertheless, photo-induced e^- and h^+ recombine quickly in ordinary substances. This recombination process can occur either in bulk or on the surface of catalyst by releasing energy in the form of unproductive heat or photons [44]. The photo-induced h^+ escaping from the pair recombination preferentially moves to the photocatalyst/electrolyte interface. The photo-induced h^+ plays an important role in generation of $^{\bullet}OH$ radicals by the trapping of adsorbed H_2O or OH^- ions from the MO dye, which has strong oxidative decomposing power in decolorization of MO dye. Meanwhile, photo-induced e^- escaping from recombination will be trapped on the surface of photocatalyst by reaction with adsorbed oxygen species to generate superoxide anion radicals ($O_2^{\bullet}$), which then will contribute to the formation of

$^{\bullet}$OH radicals by reactions with H_2O [45]. In this case, more $^{\bullet}$OH radicals will react with organic MO dye to decompose them into harmless substance.

4. Conclusion

The formation of C-TiO_2 nanotubes via single step electrochemical anodization technique successfully formed self-aligned and high-uniformity C-TiO_2 nanotube arrays with diameter of ~75 nm and length of ~2 μm with a minimal applied voltage of 30 V. The applied voltage played an important role in enhancing the field-assisted oxidation rate and field-assisted dissolution rate. The reduction of band gap energy level of C-TiO_2 nanotube arrays (3.2 eV to 2.3 eV) was due to the mixing states of the delocalized C 2p and O 2p. In photocatalytic evaluation, it was found that C-TiO_2 synthesized at 30 V exhibited the highest decolorization rate under solar irradiation among samples. The reason was mainly attributed to higher active surface area and higher uniformity of nanotube arrays has better photons absorption from solar illumination to trigger more photo-induced charge carriers for decolorization of MO dye.

Acknowledgment

The authors would like to thank Universiti Malaya for sponsoring this work under UMRG Grant (RP022-2012D).

References

[1] M. Kitano, M. Matsuoka, M. Ueshima, and M. Anpo, "Recent developments in titanium oxide-based photocatalysts," *Applied Catalysis A*, vol. 325, no. 1, pp. 1–14, 2007.

[2] H. J. Oh, J. H. Lee, Y. J. Kim, S. J. Suh, J. H. Lee, and C. S. Chi, "Synthesis of effective titania nanotubes for wastewater purification," *Applied Catalysis B*, vol. 84, no. 1-2, pp. 142–147, 2008.

[3] D. Mohan and C. U. Pittman Jr., "Arsenic removal from water/wastewater using adsorbents-A critical review," *Journal of Hazardous Materials*, vol. 142, no. 1-2, pp. 1–53, 2007.

[4] Y. C. Nah, I. Paramasivam, and P. Schmuki, "Doped TiO_2 and TiO_2 nanotubes: synthesis and applications," *ChemPhysChem*, vol. 11, no. 13, pp. 2698–2713, 2010.

[5] D. A. Tryk, A. Fujishima, and K. Honda, "Recent topics in photoelectrochemistry: achievements and future prospects," *Electrochimica Acta*, vol. 45, no. 15-16, pp. 2363–2376, 2000.

[6] A. Fujishima, X. Zhang, and D. A. Tryk, "TiO_2 photocatalysis and related surface phenomena," *Surface Science Reports*, vol. 63, no. 12, pp. 515–582, 2008.

[7] C. W. Lai and S. Sreekantan, "Preparation of hybrid WO_3-TiO_2 nanotube photoelectrodes using anodization and wet impregnation: improved water-splitting hydrogen generation performance," *International Journal of Hydrogen Energy*, vol. 38, no. 5, pp. 2156–2166, 2013.

[8] A. Kubacka, M. Fernández-García, and G. Colón, "Advanced nanoarchitectures for solar photocatalytic applications," *Chemical Reviews*, vol. 112, no. 3, pp. 1555–1614, 2012.

[9] C. A. Grimes, "Synthesis and application of highly ordered arrays of TiO_2 nanotubes," *Journal of Materials Chemistry*, vol. 17, no. 15, pp. 1451–1457, 2007.

[10] C. W. Lai and S. Sreekantan, "Incorporation of WO_3 species into TiO_2 nanotubes via wet impregnation and their water-splitting performance," *Electrochimica Acta*, vol. 87, pp. 294–302, 2013.

[11] Z. Su and W. Zhou, "Formation, morphology control and applications of anodic TiO_2 nanotube arrays," *Journal of Materials Chemistry*, vol. 21, no. 25, pp. 8955–8970, 2011.

[12] L. M. Sikhwivhilu, S. Mpelane, B. W. Mwakikunga, and S. S. Ray, "Photoluminescence and hydrogen gas-sensing properties of titanium dioxide nanostructures synthesized by hydrothermal treatments," *ACS Applied Materials and Interfaces*, vol. 4, no. 3, pp. 1656–1665, 2012.

[13] S. Sreekantan and L. C. Wei, "Study on the formation and photocatalytic activity of titanate nanotubes synthesized via hydrothermal method," *Journal of Alloys and Compounds*, vol. 490, no. 1-2, pp. 436–442, 2010.

[14] X. Chen and S. S. Mao, "Titanium dioxide nanomaterials: synthesis, properties, modifications and applications," *Chemical Reviews*, vol. 107, no. 7, pp. 2891–2959, 2007.

[15] S. Li, G. Zhang, D. Guo, L. Yu, and W. Zhang, "Anodization fabrication of highly ordered TiO_2 nanotubes," *Journal of Physical Chemistry C*, vol. 113, no. 29, pp. 12759–12765, 2009.

[16] C. W. Lai and S. Sreekantan, "Study of WO_3 incorporated C–TiO_2 nanotubes for efficient visible light driven water splitting performance," *Journal of Alloys and Compounds*, vol. 547, pp. 43–50, 2013.

[17] H. Y. Chang, W. J. Tzeng, and S. Y. Cheng, "Modification of TiO_2 nanotube arrays by solution coating," *Solid State Ionics*, vol. 180, no. 11–13, pp. 817–821, 2009.

[18] A. V. Rupa, D. Manikandan, D. Divakar, and T. Sivakumar, "Effect of deposition of Ag on TiO_2 nanoparticles on the photodegradation of Reactive Yellow-17," *Journal of Hazardous Materials*, vol. 147, no. 3, pp. 906–913, 2007.

[19] R. Taziwa, E. L. Meyer, E. Sideras-Haddad, R. M. Erasmus, E. Manikandan, and B. W. Mwakikunga, "Effect of carbon modification on the electrical, structural, and optical properties of TiO_2 electrodes and their performance in labscale dye-sensitized Solar Cells," *International Journal of Photoenergy*, vol. 2012, Article ID 904323, 9 pages, 2012.

[20] M. Paulose, H. E. Prakasam, O. K. Varghese et al., "TiO_2 nanotube arrays of 1000 μm length by anodization of titanium foil: phenol red diffusion," *Journal of Physical Chemistry C*, vol. 111, no. 41, pp. 14992–14997, 2007.

[21] C. Di Valentin, G. Pacchioni, and A. Selloni, "Theory of carbon doping of titanium dioxide," *Chemistry of Materials*, vol. 17, no. 26, pp. 6656–6665, 2005.

[22] K. Shankar, G. K. Mor, H. E. Prakasam et al., "Highly-ordered TiO_2 nanotube arrays up to 220 μm in length: use in water photoelectrolysis and dye-sensitized solar cells," *Nanotechnology*, vol. 18, no. 6, Article ID 065707, 2007.

[23] C. W. Lai and S. Sreekantan, "Optimized sputtering power to incorporate WO_3 into C–TiO_2 nanotubes for highly visible photoresponse performance," *NANO*, vol. 7, no. 6, Article ID 1250051, 8 pages, 2012.

[24] X. Yang, C. Cao, L. Erickson, K. Hohn, R. Maghirang, and K. Klabunde, "Synthesis of visible-light-active TiO_2-based photocatalysts by carbon and nitrogen doping," *Journal of Catalysis*, vol. 260, no. 1, pp. 128–133, 2008.

[25] S. Sreekantan, L. C. Wei, and Z. Lockman, "Extremely fast growth rate of TiO_2 nanotube arrays in electrochemical bath containing H_2O_2," *Journal of the Electrochemical Society*, vol. 158, no. 12, pp. C397–C402, 2011.

[26] C. W. Lai, S. Sreekantan, and Z. Lockman, "Photoelectrochemical behaviour of uniform growth TiO_2 nanotubes via bubble blowing synthesised in ethylene glycol with hydrogen peroxide," *Journal of Nanoscience and Nanotechnology*, vol. 12, no. 5, pp. 4057–4066, 2012.

[27] C. W. Lai and S. Sreekantan, "Photoelectrochemical performance of smooth TiO_2 nanotube arrays: effect of anodization temperature and cleaning methods," *International Journal of Photoenergy*, vol. 2012, Article ID 356943, 11 pages, 2012.

[28] S. K. Mohapatra, M. Misra, V. K. Mahajan, and K. S. Raja, "Design of a highly efficient photoelectrolytic cell for hydrogen generation by water splitting: application of $TiO_{2-x}C_x$ nanotubes as a photoanode and Pt/TiO_2 nanotubes as a cathode," *Journal of Physical Chemistry C*, vol. 111, no. 24, pp. 8677–8685, 2007.

[29] N. K. Allam, K. Shankar, and C. A. Grimes, "Photoelectrochemical and water photoelectrolysis properties of ordered TiO_2 nanotubes fabricated by Ti anodization in fluoride-free HCl electrolytes," *Journal of Materials Chemistry*, vol. 18, no. 20, pp. 2341–2348, 2008.

[30] C. W. Lai and S. Sreekantan, "Higher water splitting hydrogen generation rate for single crystalline anatase phase of TiO_2 nanotube arrays," *European Physical Journal*, vol. 59, no. 2, Article ID 20403, 8 pages, 2012.

[31] D. Regonini, A. Jaroenworaluck, R. Stevens, and C. R. Bowen, "Effect of heat treatment on the properties and structure of TiO_2 nanotubes: phase composition and chemical composition," *Surface and Interface Analysis*, vol. 42, no. 3, pp. 139–144, 2010.

[32] G. K. Mor, O. K. Varghese, M. Paulose, K. Shankar, and C. A. Grimes, "A review on highly ordered, vertically oriented TiO_2 nanotube arrays: fabrication, material properties, and solar energy applications," *Solar Energy Materials and Solar Cells*, vol. 90, no. 14, pp. 2011–2075, 2006.

[33] C. W. Lai and S. Sreekantan, "Heat treatment effects of WO_3-loaded TiO_2 nanotubes with enhanced water splitting hydrogen generation," *Materials Science in Semiconductor Processing*, vol. 16, pp. 947–954, 2013.

[34] B. Liu, L. Wen, and X. Zhao, "The photoluminescence spectroscopic study of anatase TiO_2 prepared by magnetron sputtering," *Materials Chemistry and Physics*, vol. 106, no. 2-3, pp. 350–353, 2007.

[35] D. Kim, J. Hong, Y. R. Park, and K. J. Kim, "The origin of oxygen vacancy induced ferromagnetism in undoped TiO_2," *Journal of Physics*, vol. 21, no. 19, Article ID 195405, 2009.

[36] Y. Zhao, Y. Li, C. W. Wang et al., "Carbon-doped anatase TiO_2 nanotube array/glass and its enhanced photocatalytic activity under solar light," *Solid State Sciences*, vol. 15, pp. 53–59, 2013.

[37] A. K. L. Sajjad, S. Shamaila, B. Tian, F. Chen, and J. Zhang, "One step activation of WO_x/TiO_2 nanocomposites with enhanced photocatalytic activity," *Applied Catalysis B*, vol. 91, no. 1-2, pp. 397–405, 2009.

[38] C. W. Lai and S. Sreekantan, "Effect of applied potential on the formation of self-organized TiO_2 nanotube arrays and its photoelectrochemical response," *Journal of Nanomaterials*, vol. 2011, Article ID 142463, 7 pages, 2011.

[39] S. Bauer, S. Kleber, and P. Schmuki, "TiO_2 nanotubes: tailoring the geometry in H_3PO_4/HF electrolytes," *Electrochemistry Communications*, vol. 8, no. 8, pp. 1321–1325, 2006.

[40] H.-C. Liang and X.-Z. Li, "Effects of structure of anodic TiO_2 nanotube arrays on photocatalytic activity for the degradation of 2,3-dichlorophenol in aqueous solution," *Journal of Hazardous Materials*, vol. 162, no. 2-3, pp. 1415–1422, 2009.

[41] Y. K. Lai, J. Y. Huang, H. F. Zhang et al., "Nitrogen-doped TiO_2 nanotube array films with enhanced photocatalytic activity under various light sources," *Journal of Hazardous Materials*, vol. 184, no. 1–3, pp. 855–863, 2010.

[42] J. M. Macak, H. Tsuchiya, A. Ghicov et al., "TiO_2 nanotubes: self-organized electrochemical formation, properties and applications," *Current Opinion in Solid State and Materials Science*, vol. 11, no. 1-2, pp. 3–18, 2007.

[43] S. Ahmed, M. G. Rasul, W. N. Martens, R. Brown, and M. A. Hashib, "Heterogeneous photocatalytic degradation of phenols in wastewater: a review on current status and developments," *Desalination*, vol. 261, no. 1-2, pp. 3–18, 2010.

[44] M. Ni, M. K. H. Leung, D. Y. C. Leung, and K. Sumathy, "A review and recent developments in photocatalytic water-splitting using TiO_2 for hydrogen production," *Renewable and Sustainable Energy Reviews*, vol. 11, no. 3, pp. 401–425, 2007.

[45] P. Roy, S. Berger, and P. Schmuki, "TiO_2 nanotubes: synthesis and applications," *Angewandte Chemie International Edition*, vol. 50, no. 13, pp. 2904–2939, 2011.